

RESEARCH ARTICLE OPEN ACCESS

FABP7 Expression Modulates the Response of Astrocytes to Induced Endotoxemia

Mariana Bresque¹  | Daniel Esteve¹  | Garret Balmer¹ | Haylee L. Hamilton² | Joshua S. Stephany¹ | Mariana Pehar^{2,3}  | Marcelo R. Vargas¹ 

¹Department of Neurology, University of Wisconsin-Madison, Madison, Wisconsin, USA | ²Division of Geriatrics and Gerontology, Department of Medicine, University of Wisconsin-Madison, Madison, Wisconsin, USA | ³Geriatric Research Education Clinical Center, Veterans Affairs Medical Center, Madison, Wisconsin, USA

Correspondence: Marcelo R. Vargas (mvargas@wisc.edu)

Received: 16 October 2024 | **Revised:** 1 April 2025 | **Accepted:** 7 April 2025

Funding: This work was supported by the National Institutes of Health, R01NS122973, R01NS132760.

Keywords: astrocytes | inflammation | LPS | microglia | NF- κ B

ABSTRACT

Fatty acid binding proteins (FABPs) are a family of small proteins involved in fatty acid (FA) subcellular trafficking. In the adult central nervous system, FABP7, one of the members of this family, is highly expressed in astrocytes and participates in lipid metabolism, regulation of gene expression, and energy homeostasis. Reactive astrocytes in Alzheimer's disease and amyotrophic lateral sclerosis animal models upregulate FABP7 expression. This upregulation may contribute to the pro-inflammatory phenotype that astrocytes display during neurodegeneration and is detrimental for co-cultured neurons. Here, we explore how FABP7 expression modulates astrocyte response to inflammatory stimuli. Our results showed that silencing FABP7 expression in astrocyte cultures before treatment with different inflammatory stimuli decreases the expression of a luciferase reporter expressed under the control of NF- κ B -response elements. Correspondingly, FABP7-silenced astrocytes display decreased nuclear translocation of the NF- κ B-p65 subunit in response to these stimuli. Moreover, silencing FABP7 decreases the toxicity of stimulated astrocytes toward co-cultured motor neurons. Similar results were obtained after silencing FABP7 in human astrocytes differentiated from induced pluripotent stem cells. Finally, knockdown of astrocytic FABP7 expression in vivo reduces glial activation in the cerebral cortex of mice after systemic bacterial lipopolysaccharide (LPS) administration. In addition, whole transcriptome RNA sequencing analysis from the cerebral cortex of LPS-treated mice showed a differential inflammatory transcriptional profile, with attenuation of NF- κ B-dependent transcriptional response after FABP7 knockdown. Together, our results highlight the potential of FABP7 as a target to modulate neuroinflammation in the central nervous system.

1 | Introduction

The connection between neuroinflammation and neurodegeneration remains difficult to define, but neuroinflammation has long been associated with the progressive nature of neurodegenerative diseases (Ransohoff 2016). The innate immune response of the central nervous system (CNS) involves a complex multicellular reaction characterized by the presence of vascular changes and infiltration of immune cells, together with activation of

resident glial cells and the production of immune and glial mediators. Neuroinflammation occurs in response to different stimuli, including aging, infection, or neurodegenerative diseases (DiSabato et al. 2016; Patani et al. 2023). Neuroinflammation in diseases such as Alzheimer's Disease (AD), Parkinson's Disease, and amyotrophic lateral sclerosis (ALS) involves a sharp phenotypic transformation of glial cells (Yang and Zhou 2019). For astrocytes, this transformation most likely represents a continuum of potential phenotypes that affect neuronal function

This is an open access article under the terms of the [Creative Commons Attribution-NonCommercial-NoDerivs](https://creativecommons.org/licenses/by-nc-nd/4.0/) License, which permits use and distribution in any medium, provided the original work is properly cited, the use is non-commercial and no modifications or adaptations are made.

© 2025 The Author(s). *GLIA* published by Wiley Periodicals LLC.

and survival in a disease-specific manner (Sofroniew 2020). However, in chronic neurological diseases, persistent neuroinflammation appears to have an overall detrimental effect on neuronal health.

The bacterial endotoxin lipopolysaccharide (LPS) is a known trigger of inflammation. Systemic LPS injections have been widely used to induce experimental neuroinflammation without directly compromising CNS structures (da Silva et al. 2024; Qin et al. 2007). Intraperitoneal LPS injections induce microglia and astrocyte reactivity, as well as nuclear factor kappa B (NF- κ B) activation and pro-inflammatory cytokine expression in the brain (Catorce and Gevorkian 2016). Systemic cytokine production is likely the primer for microglia activation observed with this treatment, which in turn leads to astrocyte activation (Zamanian et al. 2012). However, astrocytes are not just passive players in innate immunity, and bidirectional communication between astrocytes and microglia is crucial to modulate neuroinflammation. This crosstalk occurs through several mediators, including proinflammatory cytokines (IL-1 β , IL-6, and TNF α), chemokines (CCL2, CCL5, CXCL10), secondary messengers (nitric oxide and prostaglandins), and reactive oxygen species (DiSabato et al. 2016; Linnerbauer et al. 2020). Due to the role of glial cells in CNS homeostasis, it is not surprising that dysregulation of this crosstalk in response to damage or neurodegeneration may result in an environment that negatively affects neuronal health.

Fatty acid binding proteins (FABPs) are key regulators of lipid metabolism, energy homeostasis, and inflammation. They exhibit high-affinity reversible binding to saturated and/or unsaturated long-chain fatty acids as well as other lipids (Storch and Thumser 2010; Thumser et al. 2014). Many endogenous metabolites bound by the FABPs are activating ligands for peroxisome proliferator-activated receptors (PPARs), and the expression of FABPs modulates ligand-dependent PPAR-mediated transcriptional regulation (Huang et al. 2002; Hughes et al. 2015; Makowski et al. 2005; Mita et al. 2010; Tan et al. 2002; Wolfrum et al. 2001). FABPs selectively cooperate with PPARs to regulate transcription (Kannan-Thulasiraman et al. 2010; Levi et al. 2015; Tan et al. 2002; Wolfrum et al. 2001; Yu et al. 2014). However, in certain scenarios, FABPs expression can limit the activity of all three PPAR isotypes (Garin-Shkolnik et al. 2014; Helledie et al. 2000; Makowski et al. 2005). FABP7, which expression largely becomes restricted to astrocytes and radial glia-like cells in adulthood (Kurtz et al. 1994; Owada et al. 1996; Yun et al. 2012), is upregulated in astrocytes from ALS and AD animal models (Hamilton et al. 2024b; Killoy et al. 2020). In samples from AD patients and AD animal models, astrocytes surrounding amyloid plaques displayed increased FABP7 expression when compared to non-plaque-associated astrocytes (Hamilton et al. 2024b).

FABP7 up-regulation in mouse primary astrocytes as well as in human induced pluripotent stem cells (iPSCs)-derived astrocytes induces a pro-inflammatory phenotype that is detrimental to co-cultured neuronal cells (Hamilton et al. 2024b; Killoy et al. 2020). FABP7 over-expression in non-transgenic astrocytes stimulates the expression of a reporter under the control of an NF- κ B-driven promoter, as well as the expression of pro-inflammatory genes known to be regulated by NF- κ B

(e.g., *Cxcl10*, *Nos2*, among others) (Hamilton et al. 2024b; Killoy et al. 2020). Moreover, FABP7 over-expression leads to an increase in NF- κ B occupancy in the promoters of *Cxcl10* and *Nos2* genes (Killoy et al. 2020), suggesting that FABP7 up-regulation directly promotes an NF- κ B-driven pro-inflammatory response in astrocytes. Overall, while the exact mechanisms by which changes in FABP7 expression may contribute to neuroinflammation remain to be elucidated, the evidence so far indicates that FABP7 expression levels markedly alter the biology of astrocytes, as well as the way these cells interact with neighboring cells.

While FABP7 upregulation seems to favor the acquisition of a pro-inflammatory phenotype, decreasing FABP7 expression in primary astrocyte cultures isolated from symptomatic ALS mouse models reduces the expression of inflammatory markers (Killoy et al. 2020). In this study, we explored whether FABP7 expression plays a role in regulating the response of astrocytes to known inflammatory stimuli. In addition, we evaluated the therapeutic potential of knocking down FABP7 expression to modulate neuroinflammation in a well-established experimental mouse model of endotoxemia. Together, our results highlight the potential of FABP7 as a target to modulate neuroinflammation in the central nervous system.

2 | Materials and Methods

2.1 | Reagents

All chemicals and reagents were from Sigma-Aldrich unless otherwise specified. Culture media and supplements were from ThermoFisher Scientific unless otherwise specified. Primer sequences for real-time PCR analysis were previously described (Killoy et al. 2020) and were obtained from Integrated DNA Technologies.

2.2 | Astrocyte Cultures and Astrocyte-Motor Neuron Co-Cultures

Primary mouse astrocyte cultures were prepared from 1-day-old pups according to the procedure of Saneto and De Vellis (Saneto and de Vellis 1987). When confluent, cultures were shaken for 48 h at 250 rpm at 37°C, followed by a 48 h treatment with 10 μ M cytosine arabinoside. Forty-eight hours after cytosine removal, cells were re-plated at a density of 2×10^4 cells/cm². Experiments were performed when cultures reached confluency.

The iPSC line was obtained from the NINDS Human Cell and Data Repository (iPSC ID# FA0000011, control). iPSCs were differentiated into induced NPCs using an embryoid body formation protocol in the presence of SMAD signaling inhibitors (STEMdiff SMADi Media, Stemcell). Induction was confirmed by an increase in *MAP2*, *PAX6*, and *NESTIN* gene expression and a concurrent decrease in *SOX2*, *OCT3*, and *NANOG* expression. Induced NPCs were cultured for 3 weeks in astrocyte differentiation media (STEMdiff Astrocyte Differentiation Media, Stemcell), followed by 3 weeks in astrocyte maturation media (STEMdiff Astrocyte Maturation Media, Stemcell). Astrocyte differentiation was confirmed by assessing *GFAP*, *S100B*, and

ALDH1L1 gene expression, as previously shown (Hamilton et al. 2024b). Following differentiation, induced astrocytes were cultured in DMEM-F12 supplemented with 10% FBS and 0.3% N2 supplement.

Motor neuron cultures were prepared from 12.5-embryonic-day mouse spinal cords, as previously described (Harlan et al. 2016). For co-culture experiments, motor neurons were plated on primary astrocyte monolayers at a density of 300 cells/cm² and maintained for 72 h in L15 medium supplemented with 0.63 mg/mL bicarbonate, 5 µg/mL insulin, 0.1 mg/mL conalbumin, 0.1 mM putrescine, 30 nM sodium selenite, 20 nM progesterone, 20 mM glucose, 100 IU/mL penicillin, 100 µg/mL streptomycin, and 2% horse serum. Motor neurons in co-cultures with mouse primary astrocytes were identified by immunostaining against β III Tubulin (Millipore, 05-559) and survival was determined by counting all cells displaying intact neurites longer than 4 cell bodies in diameter. Counts were performed over an area of 0.90 cm² in 24-well plates. Neurite length and neurite branching were determined using the Neurotrack analysis software module on an Incucyte S3 instrument (Sartorius). Co-cultures involving iPSCs-derived astrocytes and embryonic motor neurons were performed as previously described (Killoy et al. 2022).

2.3 | Viral Vectors and Cell Treatments

An adenovirus (Ad) expressing a miR-30-based *Fabp7* shRNA embedded within the 3' UTR of a *Gfp* open reading frame under the control of the mouse *Gfap* promoter was used. The mouse *Fabp7* target sequence used was: 5'-TGTGTTACTCCAAGCAATTC-3'. The same expression cassette was used to generate AAV of the PHP.eB serotype. To silence *Fabp7* in human induced-astrocytes, an Ad expressing an shRNA under a U6 promoter was used. The human *Fabp7* target sequence used was: 5'-GTGACCAAACCAACGGTAATT-3'. All viral vectors were produced by VectorBuilder. Confluent cultures were transduced at a multiplicity of infection (MOI) of 25, 7 days prior to stimuli treatments. With this MOI we observed a 59.4% \pm 8.2 transduction efficiency as determined by the number of GFP+ cells after immunostaining. On the seventh day, astrocytes were treated with LPS (1 µg/mL, *E. coli* O55:B5, Sigma), TNF α (50 ng/mL, ThermoFisher) or a combination of IL1 α (3 ng/mL, Sigma), TNF α (30 ng/mL) and C1q (400 ng/mL, Sigma). Twenty-four hours later, astrocytes were harvested and analyzed or used for co-cultures. To analyze NF- κ B nuclear translocation, cultures were analyzed 2 h after treatment with the different inflammatory stimuli.

2.4 | Real-Time PCR and Western Blot Analysis

RNA extraction, RNA retrotranscription, real-time PCR and western blot analysis were performed as previously described (Harlan et al. 2019). Membranes were incubated overnight with one of the following antibodies: FABP7 (ThermoFisher, PA5-24949), ACTIN (Sigma, A5441), TUBULIN (Sigma, T6199), NF- κ B p65 antibody (Cell Signaling, 8242) or H3 (Cell Signaling, 4499). Image acquisition was performed in a chemiluminescent western blot scanner (Li-Cor). Quantifications were performed using the Image Studio Software (Li-Cor).

2.5 | NF- κ B Reporter Assay

Adenovirus expressing a firefly luciferase gene under the control of a synthetic promoter that contains direct repeats of the NF- κ B binding site (Ad-NF κ B-Luc) or a *Renilla* luciferase under a constitutive promoter (Ad-pRL-Luc) was obtained from Vector Biolabs. Transductions of astrocytes and luciferase assays were performed as previously described (Killoy et al. 2020).

2.6 | Animal Treatments

Experiments were performed in C57BL/6J mice (Strain #:000664; The Jackson Laboratory). At 21 days, mice received 5 \times 10¹³ vg/kg of an AAV-PHP.eB-Gfap-GFP-shFABP7 or control AAV-PHP.eB-Gfap-GFP-shScr vector. Four months later, systemic inflammation was induced with consecutive LPS injections (1 mg/kg, *E. coli* O55:B5, Sigma) for 3 weeks (one injection per week). Tissue harvesting was performed at the same time of day for all animals in this study. All animal procedures were carried out in strict accordance with the recommendations in the Guide for the Care and Use of Laboratory Animals of the NIH. The Animal Care and Use Committee of UW-Madison approved the animal protocol pertinent to the experiments reported in this work.

2.7 | Immunofluorescence

Antigen retrieval and staining in paraffin embedded tissues was performed as previously described (Harlan et al. 2020). Mouse brain sections were stained with anti-GFAP (Novus, NBP2-29415), anti-GFAP (ThermoScientific, PA5-18598), anti-IBA1 (FUJIFILM, 013-27691) or anti-GFP (Proteintech, 66002-1) antibodies. Nuclei were counterstained with DAPI (4',6-Diamidino-2-phenylindole dihydrochloride). Co-immunostaining images of GFAP and IBA1 were captured using a Nikon A1R-Si+ confocal microscope. The same cortical area was chosen for analysis in all mice and experimental conditions. We obtained sequential 20 µm sagittal brain sections starting at the medial line, and the same section number from each animal was processed for staining. The shape of the hippocampal formation was used to confirm the same sagittal plane was analyzed for each animal. Following staining, 60X images covering an area of 0.15 mm² were acquired in layer 2/3 of the cerebral cortex located above the hippocampal formation, using the dentate gyrus as an initial reference. For GFAP and IBA1 quantification, images were acquired with identical settings at a z-stack step size of 0.5 µm. Fluorescence intensity quantification was performed using the National Institute of Health Fiji (Image J) software. Using Fiji software, we obtained the maximum intensity projection of 20 Z-stack images. After subtracting the background, we applied the threshold tool to create a binary mask to identify GFAP+ areas. Finally, we measured the area fraction to establish the percentage of the image covered by GFAP staining. All images were processed with the same settings. The area occupied by the signal was calculated as a percentage of the total area analyzed. The same procedure was applied for IBA1 maximum intensity projection images. Microglia cell soma size analysis was performed in the maximum intensity projection images. Boundaries of the microglia cell body were delimited

manually excluding the projections. All microglia cell bodies were added to the region of interest manager, and their area was determined. Immunostaining in cell culture experiments was performed as previously described (Hamilton et al. 2024a), using the following antibodies: p65 NF- κ B (Cell Signaling, 8242) and β -III tubulin (Sigma-Aldrich, T8578). Nuclei were counterstained with DAPI.

2.8 | RNA Sequencing (RNA-seq) and Data Analysis

Total RNA was isolated from cortical tissue using TRI Reagent according to the manufacturer's instructions. Quality control, RNA library preparations, sequencing reactions, and initial data analysis (trimming, mapping, and differential gene expression) were performed by Azenta Life Sciences. Comparison of gene expression levels between groups was performed as previously described (Hamilton et al. 2024b). The RNA-seq data was deposited in NCBI's Gene Expression Omnibus (GEO; accession number GSE279612). Transcription factor-target interaction search was performed in the TRRUST v2 database (Han et al. 2018).

2.9 | Statistical Analysis

Groups of 3–7 animals were used for biochemical analysis and data from each animal were plotted as individual points in the graphs. Unless otherwise noted, cell culture experiments were repeated in at least three independent primary culture preparations with at least 2 technical replicates per treatment group, and values from each independent experimental replicate are plotted as individual points. All data are reported as mean \pm SD. Comparisons between two groups were performed with an unpaired t-test. Multiple group comparisons were performed by one-way ANOVA with Tukey's post-test. When comparing the effect of combinations of treatments, two-way ANOVA was used followed by Tukey's post-test. Differences were declared statistically significant if $p \leq 0.05$. All statistical computations were performed using Prism 9.0 (GraphPad Software).

3 | Results

To examine the effect of silencing FABP7 in astrocytes exposed to different inflammatory stimuli, we transduced these cells with an adenovirus (Ad) coding for a miR-30-based short hairpin (sh) RNA targeting FABP7 mRNA (shFabp7). This shFabp7 was embedded within the 3'-UTR of an expression cassette that encodes GFP protein under the control of the mouse *Gfap* promoter (Figure 1A). An identical construct expressing a scramble non-silencing shRNA (shScr) was used as a control. shFABP7 treatment decreased FABP7 expression in cortical astrocytes to approximately 40% when compared to scramble controls (Figure 1B–D), without causing morphological changes as reflected by GFAP immunostaining (Figure 1E). We then compared the magnitude of NF- κ B-driven transcriptional activation induced by proinflammatory stimuli in Ad-shScr and Ad-shFabp7 transduced astrocytes. Twenty four hours after treatment with LPS (Figure 1F), TNF α (Figure 1G), or a cocktail containing IL1 α , TNF α and C1q (Figure 1H), a significant

increase in NF- κ B-driven transcriptional activity is observed in scramble control cultures. However, decreasing FABP7 expression prior to the treatments significantly decreased NF- κ B activation (Figure 1F–H, shFabp7). The decrease observed in NF- κ B-driven transcriptional activation in FABP7-silenced cultures correlates with a significant reduction in NF- κ B-p65 nuclear translocation in those cultures (Figure 2A–F). Subcellular fractionation and western blot analysis confirmed a decrease of NF- κ B-p65 levels in the nuclear fraction of LPS stimulated astrocytes after silencing FABP7, when compared to scramble controls (Figure 2G,H).

Astrocytes promote the survival of co-cultured motor neurons but can be activated by exposure to LPS and cytokines to induce cell death (Cassina et al. 2002; Liddelow et al. 2017). The gene program and subsequently phenotypic changes downstream of NF- κ B activation in astrocytes may contribute to this observation. To examine whether the decrease in inflammatory response conferred by silencing FABP7 in activated astrocytes affects the way these cells interact with neighboring neurons, we tested the survival of motor neurons co-cultured with FABP7-silenced astrocyte cultures treated with different inflammatory stimuli. Silencing FABP7 does not alter the number of motor neurons attached to the astrocyte monolayer in control conditions (Figure 3A–C, shScr-control vs. shFabp7-control). Inflammatory stimuli-activated astrocytes induced about 25%–30% motor neuron loss, while silencing FABP7 in astrocytes before activation reverted motor neuron loss in co-cultures (Figure 3A–C). Moreover, motor neurons co-cultured with activated Ad-shFabp7-transduced astrocytes display increased neurite length and complexity, variables generally associated with neuronal health (Figure 3D–F), suggesting that silencing FABP7 may prevent deleterious effects of activated astrocytes while preserving neurotrophic functions.

To investigate if FABP7 downregulation has a similar effect in human iPSCs-derived astrocytes obtained from a healthy control subject (i-astrocytes), we analyzed NF- κ B transcriptional activation following FABP7 silencing. We used an adenovirus expressing a short hairpin RNA (shRNA) specific for human *Fabp7* or a scramble non-silencing control under a U6 promoter. Western blot analysis confirmed an approximately 40% decrease in FABP7 expression 8 days following viral transduction (Figure 4A,B). Treatment with TNF α induced expression from an NF- κ B-driven promoter in control i-astrocyte cultures. On the other hand, silencing FABP7 in i-astrocytes significantly reduced NF- κ B transcriptional activation (Figure 4C) and NF- κ B-p65 nuclear translocation (Figure 4D). Moreover, silencing FABP7 before TNF α treatment decreased the toxicity of these cells toward co-cultured motor neurons (Figure 4E).

Using a viral-mediated strategy that confers long-lasting astrocyte-specific FABP7 downregulation in vivo (Figure 5A,F), we tested the effect of modulating FABP7 expression during neuroinflammation. At 21 days of age, mice received a retro-orbital injection of an AAV-PHPeB vector that codes for an embedded non-silencing scramble (AAV-PHP.eB-Gfap-GFP-shScr) or a *Fabp7*-specific shRNA (AAV-PHP.eB-Gfap-GFP-shFABP7) under the control of a *Gfap* promoter. In agreement with previous observations that found no macroscopic abnormalities in embryonic and adult brains from

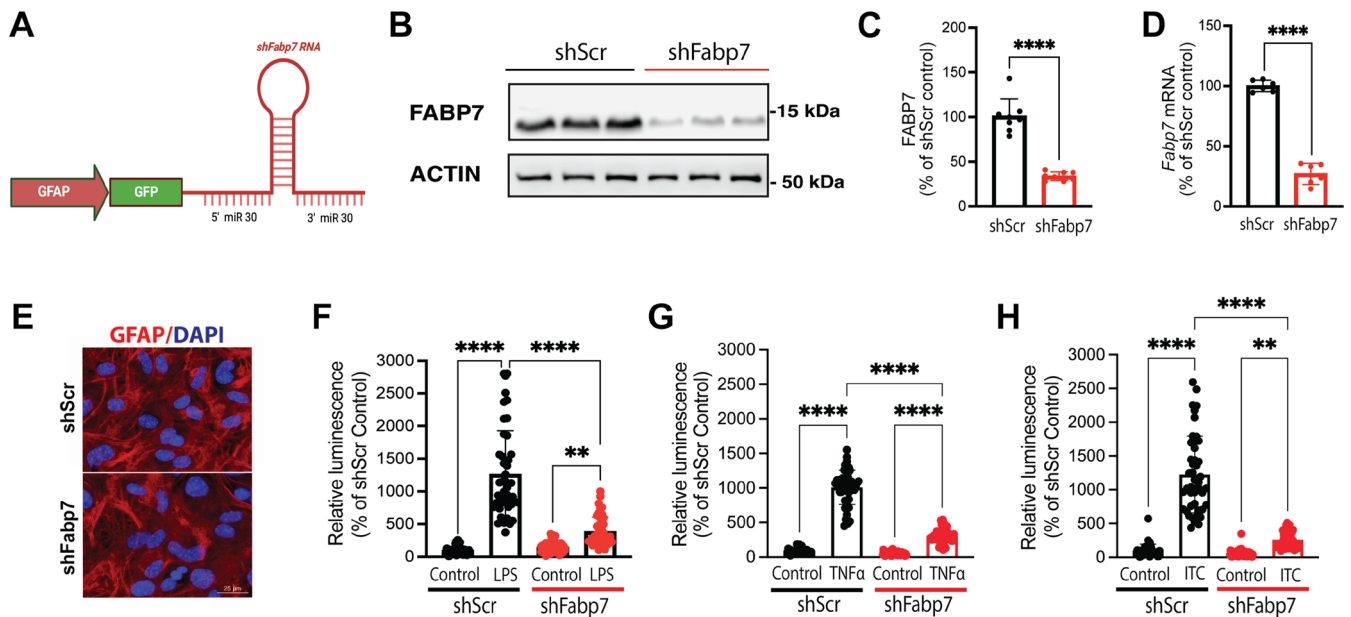


FIGURE 1 | Decreasing FABP7 expression reduces NF- κ B-driven transcriptional activity in astrocytes. Confluent mouse primary cortical astrocyte cultures were transduced with an adenovirus (Ad) expressing a short hairpin RNA (shRNA) specific for *Fabp7* (shFabp7) or a scramble non-silencing control shRNA (shScr) for 7 days. (A) Design of the shFabp7 construct expressing a miR-30-based *Fabp7* shRNA embedded within the 3'UTR of an expression cassette that encodes GFP protein under the control of the mouse *Gfap* promoter. (B) Representative Western blot analysis image of FABP7 expression in Ad-shScr and Ad-shFabp7 transduced astrocytes. (C) Quantification of FABP7 protein levels by Western blot analysis. FABP7 expression was quantified, normalized by Actin levels, and expressed as a percentage of Ad-shScr samples (mean \pm S.D.). (D) *Fabp7* mRNA levels were determined by real-time PCR and corrected by *Actin* mRNA levels. Data are expressed as a percentage of Ad-shScr samples (mean \pm S.D.). (E) Representative images of astrocyte cultures transduced with Ad-shScr (top) and Ad-shFabp7 (bottom). Astrocyte cultures were immunostained for GFAP (red). Nuclei were counterstained with DAPI (blue). Scale bar: 25 μ m. (F–H) Four days after Ad-shScr and Ad-shFabp7 transduction, astrocytes were co-transduced with a firefly luciferase construct under the control of a minimal promoter with tandem NF- κ B response elements, and a *Renilla* luciferase construct under a constitutive promoter. On day 7, treatment with inflammatory stimuli was performed. Relative luminescence produced by firefly luciferase expressed under the NF- κ B-driven promoter was measured 24 h after treatment with vehicle (PBS; control), LPS (1 μ g/mL) (F); TNF α (50 ng/mL) (G); or a cocktail containing (ITC) IL1 α (3 ng/mL), TNF α (30 ng/mL), and C1q (400 ng/mL) (H). Relative firefly luciferase luminescence was corrected by *Renilla* luciferase luminescence and expressed as a percentage of Ad-shScr-vehicle treated (control) cells. For F–H, data points represent the value obtained from individual technical replicates from at least three independent primary cultures preparations. Data are expressed as a percentage of shScr control cells ($n = 3$ –4, mean \pm S.D.). *** $p < 0.0001$, ** $p < 0.01$.

Fabp7 knockout mice (Owada et al. 2006), no gross effect on brain development was observed due to viral-mediated FABP7 silencing. At 4 months of age, animals were injected with LPS (1 mg/kg) once a week for 3 consecutive weeks and harvested 24 h after the last injection. Intraperitoneal LPS injections triggered glial reactivity as reflected by GFAP and IBA1 expression in scramble-control animals (Figures 5 and 6), while decreasing FABP7 expression attenuates glial reactivity. In control conditions, silencing FABP7 does not cause statistically significant transcriptional changes in *Gfap*, *Iba1*, and *Cxcl10* expression at 4 months of age (Figure 5B–D, control-shScr vs. control-shFabp7). On the other hand, GFAP expression and immunoreactivity were significantly downregulated in the cerebral cortex of animals that received the *Fabp7*-specific shRNA prior to the LPS challenge (Figure 5B,E,G and Figure 6A,B). In addition, *Cxcl10* mRNA expression was also reduced in this group (Figure 5D). While we did not observe a decrease in *Iba1* mRNA expression in shFABP7-LPS-treated animals (Figure 5C), IBA1 protein expression and immunoreactivity are significantly decreased in the cerebral cortex of these mice (Figures 5H,I and 6A,C). While microglia morphology cannot be interpreted as a synonymous with microglia function,

changes in microglia morphology are linked to the response of these cells to an ongoing neuroinflammatory environment (Norden et al. 2016; Perry et al. 2010); and differential changes in body size and branching likely reflect differential physiological states of these cells. Microglia soma size, process thickness, and NF κ B-p65 staining in these cells were decreased in the cerebral cortex of shFabp7-LPS-treated mice when compared to the shScr-LPS control group (Figure 7).

RNA sequencing analysis comparing differential gene expression in the cerebral cortex of AAV-shScr-LPS and AAV-shFABP7-LPS treated mice identified a total of 406 differentially expressed genes (DEG) with at least a 1.5-fold change in expression and p adjusted ≤ 0.05 (131 upregulated and 275 downregulated, Table S1). Among the downregulated DEG found, *Fabp7*, *Gfap*, and *Cxcl10* mRNA downregulation were confirmed by real-time PCR (Figure 5A,B,D). Enrichment analysis using TRRUST v2 (Han et al. 2018) identified NF κ B1 and *Rela* as the top two transcription factors potentially involved in the regulation of the DEG found in our samples (Figure 8A). It is worth noting that the most abundant form of NF- κ B is the complex formed by these two sub-units. A heatmap representing the normalized

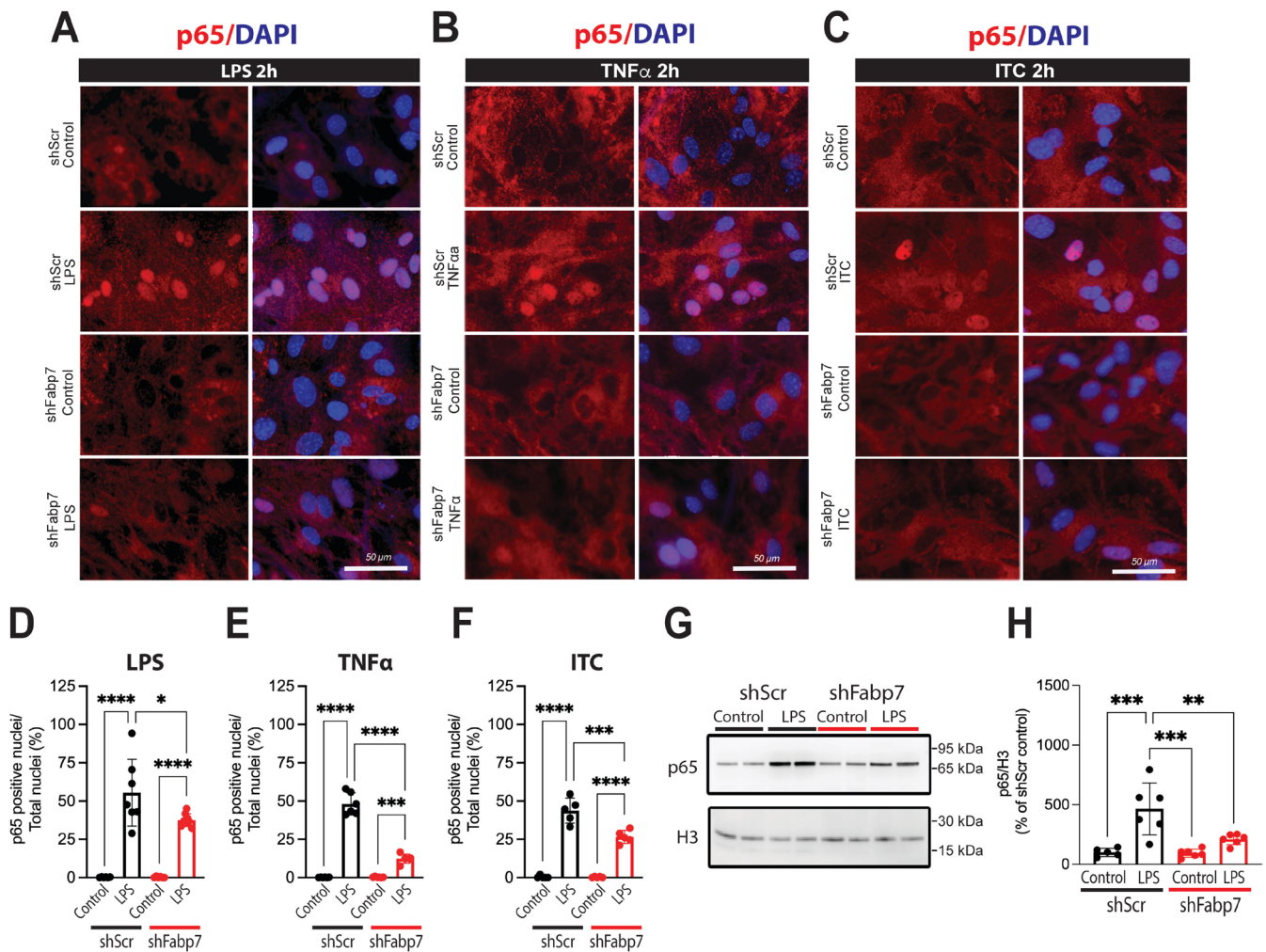


FIGURE 2 | Decreasing FABP7 expression reduces NF- κ B nuclear translocation in astrocytes. Confluent mouse primary cortical astrocyte cultures were transduced with the adenovirus (Ad) vectors described in Figure 1A, expressing a short hairpin RNA (shRNA) specific for Fabp7 (shFabp7) or a scramble non-silencing control shRNA (shScr). After 7 days, astrocytes were treated for 2 h with LPS (1 μ g/mL) (A), TNF α (50 ng/mL) (B); or a cocktail (ITC) containing IL1 α (3 ng/mL), TNF α (30 ng/mL), and C1q (400 ng/mL) (C). (A–C) Representative images of NF- κ B p65 immunostaining (red) in Ad-shScr (top panels) and Ad-shFabp7 (bottom panels) transduced astrocyte cultures. Nuclei were counterstained with DAPI (blue). Scale bar: 50 μ m. (D) Quantification of NF- κ B p65 positive nuclei in Ad-shScr and Ad-shFabp7 transduced astrocytes treated as described above with LPS. Data is expressed as a percentage of NF- κ B p65 positive nuclei over total nuclei. Each data point represents the percentage of positive nuclei per image analyzed (mean \pm S.D.). The average total number of nuclei per image was 331 \pm 57 for control-shScr; 397 \pm 61 for LPS-shScr; 372 \pm 26 for control-shFabp7; and 321 \pm 46 for LPS-shFabp7. (E) Quantification of NF- κ B p65 positive nuclei in Ad-shScr and Ad-shFabp7 transduced astrocytes treated as described above with TNF α . Data is expressed as a percentage of NF- κ B p65 positive nuclei over total nuclei. Each data point represents the percentage of positive nuclei per image analyzed (mean \pm S.D.). The average total number of nuclei per image was 422 \pm 60 for control-shScr; 401 \pm 52 for TNF α -shScr; 352 \pm 54 for control-shFabp7; and 400 \pm 68 for TNF α -shFabp7. (F) Quantification of NF- κ B p65 positive nuclei in Ad-shScr and Ad-shFabp7 transduced astrocytes treated as described above with the ITC cocktail. Data is expressed as a percentage of NF- κ B p65 positive nuclei over total nuclei. Each data point represents the percentage of positive nuclei per image analyzed (mean \pm S.D.). The average total number of nuclei per image was 164 \pm 23 for control-shScr; 154 \pm 43 for ITC-shScr; 147 \pm 16 for control-shFabp7; and 149 \pm 48 for TNF α -shFabp7. (G) Representative Western blot analysis of NF- κ B p65 expression levels in nuclear extracts from Ad-shFabp7 and Ad-shScr transduced astrocytes 2 h after LPS (1 μ g/mL) stimulation. (H) Quantification of NF- κ B p65 nuclear protein levels shown in (G). NF- κ B p65 expression was quantified, normalized by H3 levels, and expressed as a percentage of shScr control samples (mean \pm S.D.). Each data point corresponds to the value obtained from individual technical replicates from three independent experiments performed in duplicate. **** p < 0.0001, *** p < 0.001, ** p < 0.01, * p < 0.05.

expression counts for the transcripts potentially regulated by these two transcription factors is shown in Figure 8B. Most of these genes were downregulated in the cortex of shFabp7-LPS treated mice, suggesting that decreasing FABP7 also attenuates NF- κ B-mediated signaling in vivo.

4 | Discussion

Neuroinflammation could actively contribute to neurodegeneration and a better understanding of the role of the different CNS cell types involved in this process may lead to the development

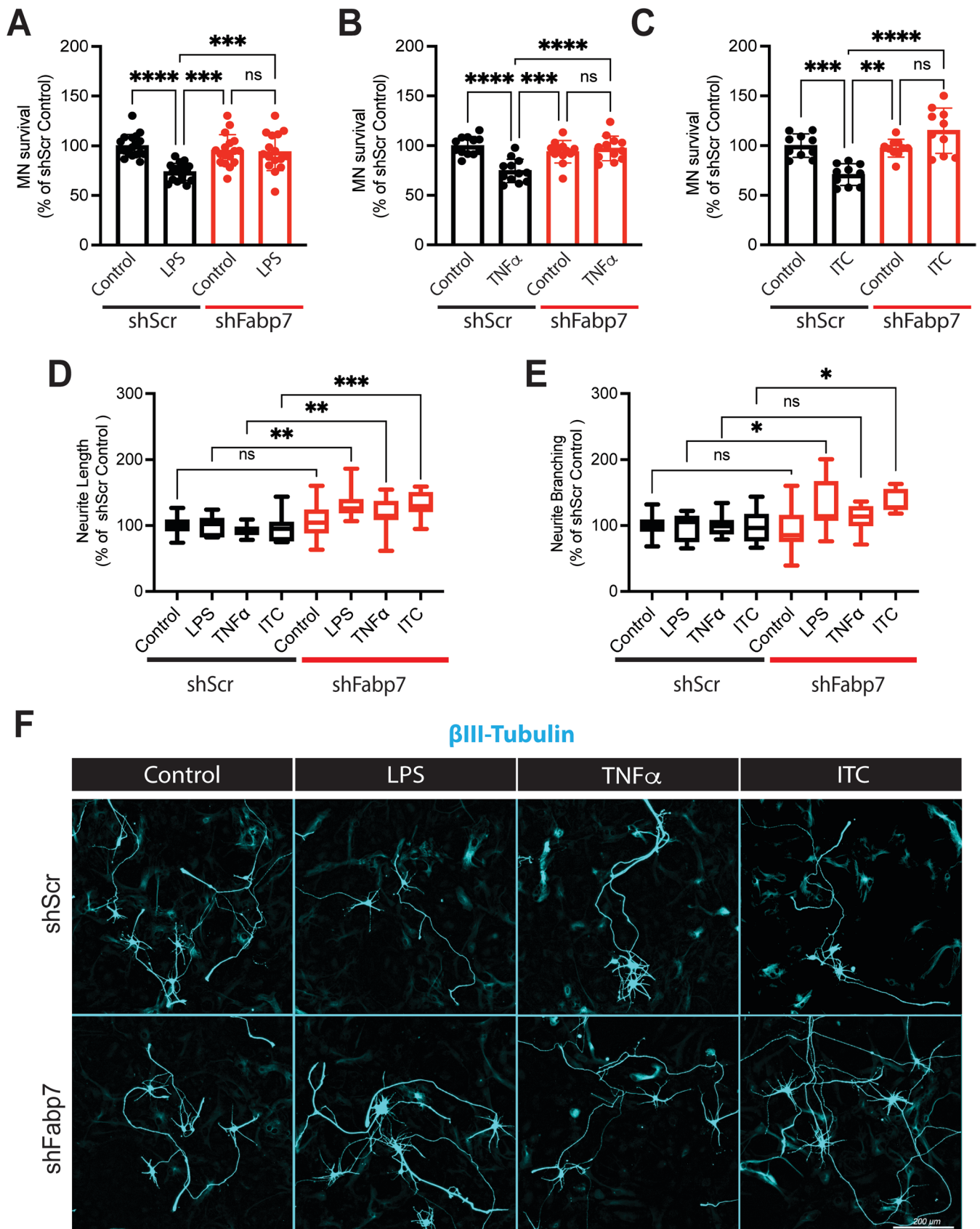


FIGURE 3 | Legend on next page.

of therapeutic strategies. We have previously shown that decreasing FABP7 expression reduces the expression of inflammatory markers in astrocytes isolated from an ALS mouse model

(Killoy et al. 2020). Since the nature and context of the triggering stimuli likely affect the response of astrocytes, it was important to explore if a similar mechanism could be relevant in

FIGURE 3 | Knockdown of FABP7 expression in activated astrocytes confers protection to co-cultured motor neurons. Confluent mouse primary cortical astrocyte cultures were transduced with an adenovirus (Ad) expressing a short hairpin RNA (shRNA) specific for Fabp7 (shFabp7) or a scramble non-silencing control shRNA (shScr) for 7 days. On day 7, astrocytes were treated with vehicle (PBS; control), LPS (1 $\mu\text{g}/\text{mL}$) (A), TNF α (50 ng/mL) (B); or a cocktail (ITC) containing IL1 α (3 ng/mL), TNF α (30 ng/mL), and C1q (400 ng/mL) (C). Twenty-four hours later purified embryonic motor neurons (MN) were plated on top of the astrocyte monolayer. MN survival was determined 72 h later. (A–C) Percentage of MN survival in co-cultures with Ad-shScr or Ad-shFabp7 transduced astrocytes and treated with pro-inflammatory stimuli as indicated above. Data are expressed as a percentage of Ad-shScr vehicle treated (control) cultures. Data were obtained from at least 3–4 independent co-culture experiments, 2–3 replicates per co-culture. ($n = 3–4$, mean \pm S.D.). (D, E) MN neurite length (D) and branching (E) in co-cultures performed as indicated above. Data are expressed as a percentage of Ad-shScr vehicle treated (control) cultures ($n = 3–4$, mean \pm S.D.). (F) Representative images of β III-Tubulin immunostaining (cyan) in co-cultures treated as indicated above. Scale bar: 200 μm . **** $p < 0.0001$, *** $p < 0.001$, ** $p < 0.01$, * $p < 0.05$.

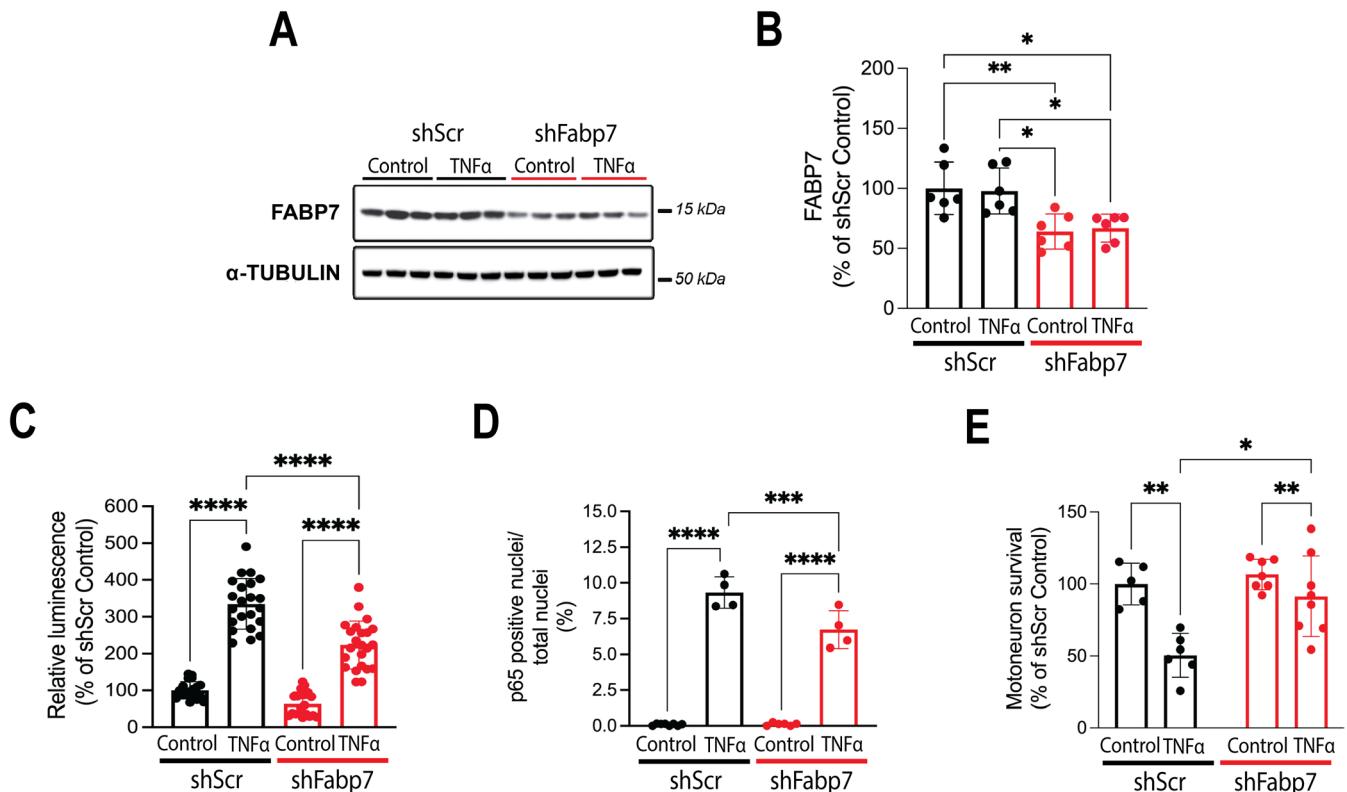


FIGURE 4 | Knockdown of FABP7 expression reduces NF- κ B activation in human iPSC-derived astrocytes (iAs) and confers protection to co-cultured motor neurons. Confluent iAs cultures were transduced with an adenovirus (Ad) expressing a short hairpin RNA (shRNA) specific for human Fabp7 (shFabp7) or a scramble non-silencing control shRNA (shScr) for 7 days. On day 7, cultures were treated with vehicle (PBS; control) or TNF α (50 ng/mL) and FABP7 levels were analyzed by western blot 24 h later. (A) Representative Western blot analysis image of FABP7 expression in Ad-shScr and Ad-shFabp7 transduced iAs. (B) Quantification of FABP7 protein levels by Western blot analysis. FABP7 expression was quantified and normalized by α -TUBULIN levels. Data are expressed as a percentage of Ad-shScr vehicle treated (control) cultures (two independent experiments performed in triplicate, mean \pm S.D.). Each data point corresponds to a replicate. (C) Confluent iAs cultures were transduced with Ad-shScr and Ad-shFabp7. Four days after Ad-shScr and Ad-shFabp7 transduction, astrocytes were co-transduced with a firefly luciferase construct under the control of a NF- κ B-driven promoter, and a *Renilla* luciferase construct under a constitutive promoter. On day 7, cultures were treated with vehicle (PBS; control) or TNF α (50 ng/mL). Relative luminescence produced by firefly luciferase was measured 24 h after treatment with TNF α (50 ng/mL) in Ad-shScr or Ad-shFabp7 transduced iAs cultures. Relative firefly luciferase luminescence was corrected by *Renilla* luciferase luminescence and expressed as a percentage Ad-shScr-vehicle treated (control) cells (data points represent the data obtained from individual wells, mean \pm S.D.). (D) Quantification of NF- κ B p65 immunostained positive nuclei in Ad-shScr and Ad-shFabp7 transduced iAs cultures treated with vehicle (PBS; control) or TNF α (50 ng/mL) for 2 h. Each data point represents the percentage of NF- κ B p65 positive nuclei over total nuclei per image analyzed (mean \pm S.D.). The average total number of nuclei per image was 743 \pm 75 for control-shScr; 708 \pm 25 for TNF α -shScr; 716 \pm 72 for control-shFabp7; and 777 \pm 86 for TNF α -shFabp7. (E) Percentage of motor neuron (MN) survival in co-cultures with Ad-shScr or Ad-shFabp7 transduced iAs treated with pro-inflammatory stimuli as indicated above. MN survival was determined after 72 h in co-culture. Data are expressed as a percentage of Ad-shScr vehicle treated (control) cultures. Data were obtained from two independent co-culture experiments, with at least 2 technical replicates per treatment group (mean \pm S.D.). **** $p < 0.0001$, *** $p < 0.001$.

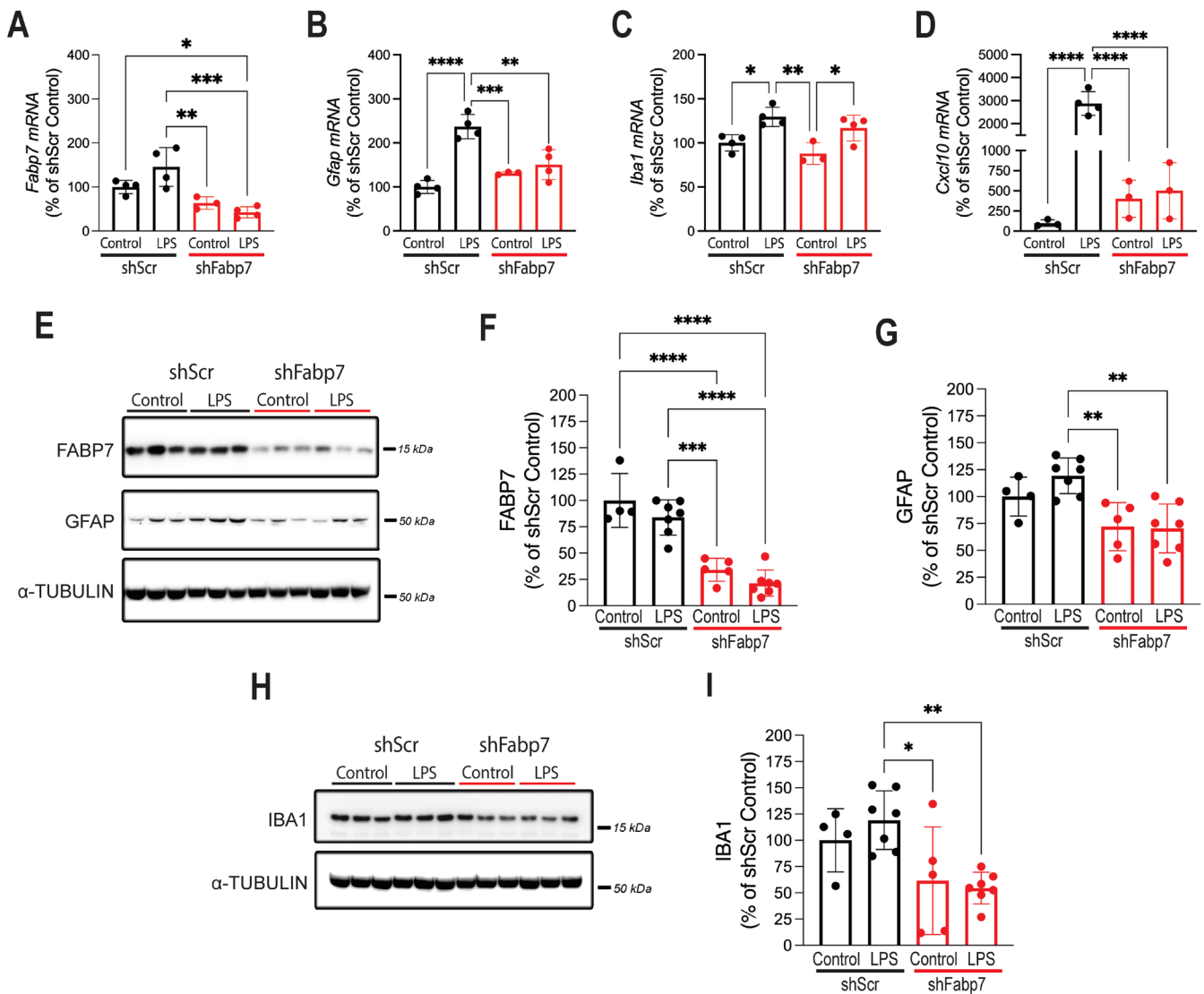


FIGURE 5 | Knockdown of FABP7 expression reduces GFAP levels in a mouse model of neuroinflammation. 21-days-old mice received a retro-orbital venous sinus injection of a control AAV-PHP.eB-Gfap-GFP-shScr (shScr) or AAV-PHP.eB-Gfap-GFP-shFABP7 (shFABP7) vector (5×10^{13} vg/kg). Four months later, systemic inflammation was induced by consecutive LPS (1 mg/kg) injections for 3 weeks (one injection per week). Control animals received vehicle injections (saline). Analysis was performed 24h after the last injection. (A–D) *Fabp7*, *Gfap*, *Iba1* and *Cxcl10* mRNA expression from brain cortical samples in AAV-shScr and AAV-shFABP7 injected mice. mRNA levels were determined by real-time PCR and corrected by *Rplp0* mRNA levels. No statistically significant differences in *Rplp0* mRNA expression were observed across all treatment groups. (E) Representative Western blot analysis of FABP7 and GFAP expression from cortical brain samples from animals treated as above. (F, G) Quantification of FABP7 and GFAP protein levels by Western blot analysis. (H) Representative Western blot analysis of IBA1 expression from cortical brain samples from animals treated as above. (I) Quantification of IBA1 expression from cortical brain samples from animals treated as above. FABP7, GFAP and IBA1 expression was quantified, normalized by TUBULIN levels. Data are expressed as a percentage of AAV-shScr vehicle treated (control) mice ($n = 3-4$ for mRNA, $n = 4-7$ for protein, mean \pm S.D.).

a model of systemic inflammation. Here we show that FABP7 expression levels regulate the response of astrocytes to inflammatory stimuli and affect their crosstalk with other cell types during neuroinflammatory processes.

Using a FABP7 specific shRNA expressed under the control of a *Gfap* promoter, we demonstrated that in response to different inflammatory stimuli, knockdown of FABP7 expression reduces NF- κ B-dependent transcriptional activity in astrocytes and reverts the toxicity of these activated cells toward co-cultured neurons. Whether astrocytes directly respond to LPS through the TLR4 receptor remains contested,

with reports showing that astrocytes in culture and in vivo express TLR4 (Gorina et al. 2011; Shen et al. 2016; Zamanian et al. 2012; Zhang et al. 2014), while others indicate that astrocytes depend on microglia to respond to TLR4 ligands such as LPS (Chen et al. 2015; Holm et al. 2012). We cannot rule out that the presence of minimal contaminating microglia in our primary cultures (less than 1%) may be mediating the response of astrocytes to LPS. Regardless of whether it is LPS or a factor released by microglia in response to LPS, the decrease in NF- κ B-mediated activation observed in these cultures after silencing FABP7 is restricted to the astrocyte compartment, since the *Gfap* promoter drives the expression of the *Fabp7*-shRNA.

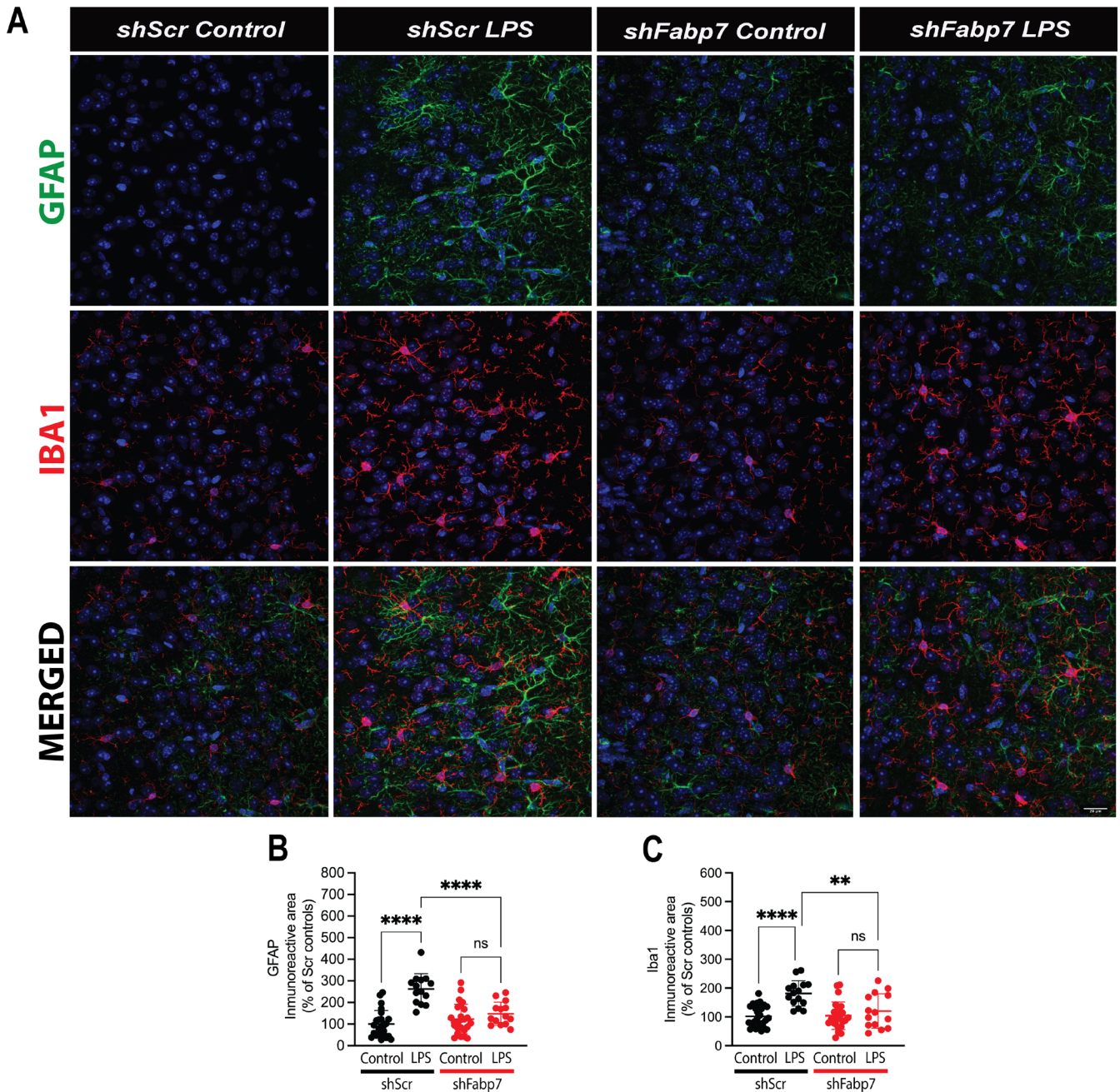


FIGURE 6 | Knockdown of FABP7 expression reduces glial activation in a mouse model of neuroinflammation. Tissue sections from animals treated as in Figure 7 were used for histological analysis. (A) Representative images showing GFAP (green) and IBA1 (red) co-immunostaining in the cerebral cortex of AAV-shScr and AAV-shFabp7 injected mice treated with vehicle (control) or LPS. Nuclei were counterstained with DAPI (blue). Scale bar: 20 μ m. (B, C) Quantification of the area occupied by GFAP (B) or IBA1 (C) positive cells in the cerebral cortex of AAV-shScr or AAV-shFABP7 injected mice treated with vehicle or LPS. At least 3 images per animal were analyzed, $n = 8$ animals/genotype for control groups and $n = 4$ animals/genotype for LPS groups; data are expressed as mean \pm SD. **** $p < 0.0001$, *** $p < 0.001$, ** $p < 0.01$, * $p < 0.05$.

Accordingly, silencing FABP7 also dampens NF- κ B activation induced by treatment with TNF α or a cocktail of cytokines that has been proposed to mediate microglia-dependent astrocyte activation (IL-1 α , TNF α , and C1q) (Liddelow et al. 2017). Thus, independently of whether the inflammatory stimulus is being directly sensed by astrocytes or involves a crosstalk with microglia, the downregulation of FABP7 expression in astrocytes attenuates the inflammatory response and reverts the acquired neurotoxic phenotype.

While the data supports a similar tempering effect of decreasing FABP7 expression in the activation of NF- κ B signaling in mouse primary astrocytes and human iPSC-derived astrocytes, the upstream events leading to this observation remain to be established. In malignant glioma cells, FABP7 plays a key role in the delivery of arachidonic acid (AA) to the endoplasmic reticulum for metabolism by COX-2 (Elsherbiny et al. 2013; Mita et al. 2010). Enhanced metabolism of AA by COXs generates 2-series prostaglandins (PGs) that have been shown to be more

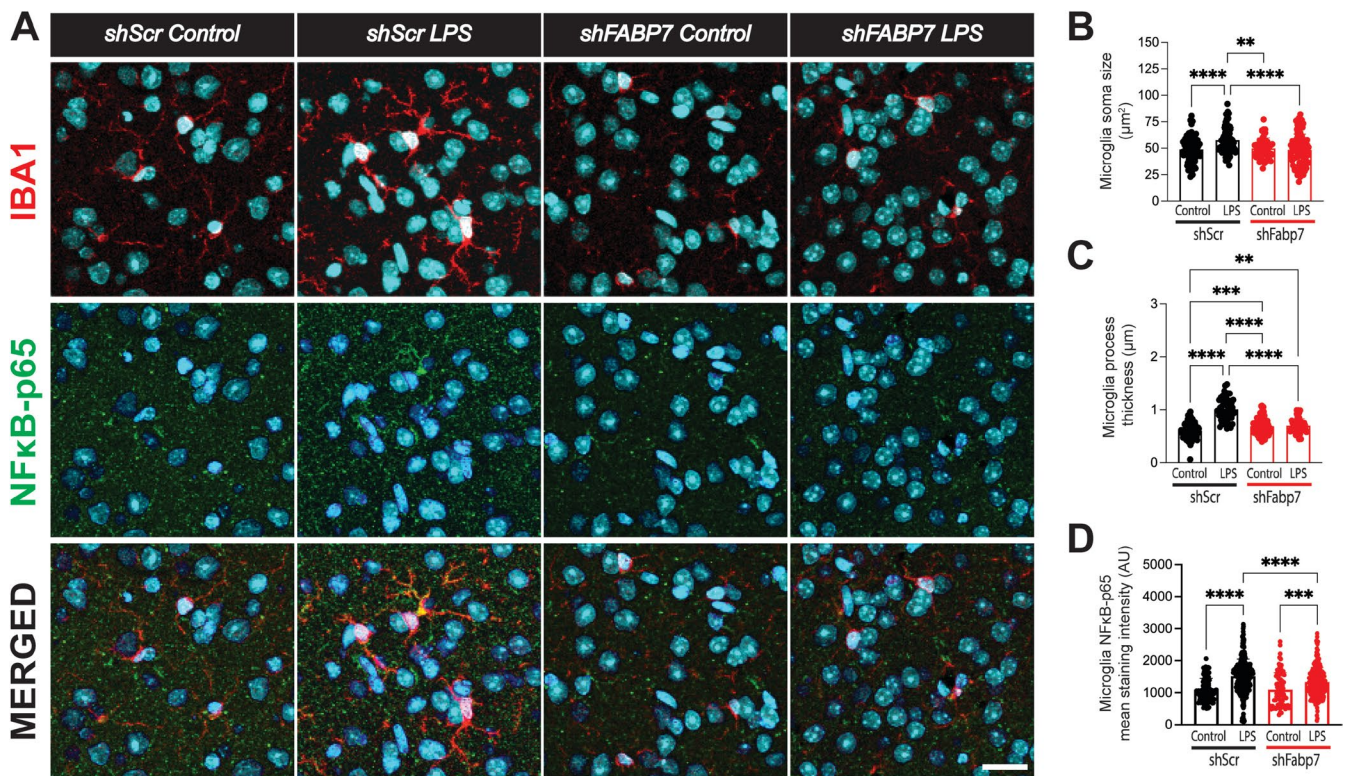


FIGURE 7 | Knockdown of FABP7 expression in astrocytes alters microglia response to LPS-induced neuroinflammation. (A) Representative images showing IBA1 and NF- κ B p65 immunostaining in the cerebral cortex of control AAV-PHP.eB-Gfap-GFP-shScr or AAV-PHP.eB-Gfap-GFP-shFABP7 vector injected mice and treated with vehicle (saline; control) or LPS, as indicated in Figure 5. Nuclei were counterstained with DAPI (cyan). Scale bar: 20 μ m. Images for each individual channel are shown in Figure S1. (B) Microglia soma size (excluding projection) determined in maximum intensity projection images from the cortex of the animals treated as above. (C) Microglia process thickness size determined in maximum intensity projection images from the cortex of the animals treated as above. (D) NF- κ B p65 immunostaining quantification in IBA1+ cells from the cortex of the animals treated as above. Data are expressed as mean \pm SD. Individual glia size and quantification was performed in at least 3 images per animal, $n=4$ animals/genotype; **** $p < 0.0001$, *** $p < 0.001$, ** $p < 0.01$, * $p < 0.05$.

proinflammatory than the 3-series PGs generated by docosahexaenoic acid (DHA) metabolism (Bagga et al. 2003). Interestingly, 2-series PGs have been shown to play an important role in the crosstalk between microglia and astrocytes in models of systemic LPS administration (Johansson et al. 2013). Since the affinity of FABP7 for DHA is higher than the affinity for AA (Balendiran et al. 2000), changes in FABP7 expression could alter the balance of PGs production in astrocytes. A decrease in FABP7 expression is expected to lower the production of all PGs. In addition, at lower levels of FABP7 expression, DHA metabolism would be favored, and therefore the ratio between 3-series:2-series PGs is expected to be higher. In addition, Kagawa et al. demonstrated that LPS-dependent TLR4 recruitment into lipid rafts, as well as the production of TNF α , was significantly decreased in FABP7 knockout astrocytes (Kagawa et al. 2015). Thus, changes in FABP7 expression may alter transmembrane receptor recruitment into lipid rafts and dampen their activation through its effect on membrane fluidity, interfering with receptor clustering.

Partial or complete ablation of astrocytic NF- κ B signaling in different models of neuroinflammation improves pathological outcomes and has been linked to decreased levels of cytokine production and glial activation (Linnerbauer et al. 2020; Ouali Alami et al. 2018). While there appears to be minimal LPS blood-brain barrier penetration (Banks and Robinson 2010), systemic LPS administration induces an inflammatory response

that likely involves microglial response to systemic cytokines and subsequent astrocyte activation (Zamanian et al. 2012). Our data show that silencing astrocytic FABP7 in a model of mild chronic inflammation decreases glial activation and NF- κ B-mediated transcriptional activity. Microglial cell response to LPS inflammation involves morphological alterations indicative of an activated state. While FABP7 is mainly expressed by astrocytes in the adult CNS and the shRNA expression is driven by a *Gfap* promoter, in shFABP7-LPS-treated animals, microglial cells display evidence of lower activation, including decreased soma size and NF- κ B-p65 staining. Bidirectional communication between astrocytes and microglia is crucial to modulating neuroinflammation, and our data suggest that silencing astrocytic FABP7 may not only restrain astrocyte response but may also influence microglia-astrocyte crosstalk.

Multiple studies have linked LPS-induced neuroinflammation to a harmful astrocytic phenotype associated with marked transcriptional profile changes (Hasel et al. 2021; Liddel et al. 2017; Zamanian et al. 2012). Hasel et al. (Hasel et al. 2021) described several subtypes of neuroinflammatory astrocytes with defined transcriptomic profiles. Although our transcriptomics data do not have cell-type resolution, 34 of the genes displaying differential expression in our study are represented in the cluster-specific LPS-responsive genes described by these authors. More importantly, 25 of them were

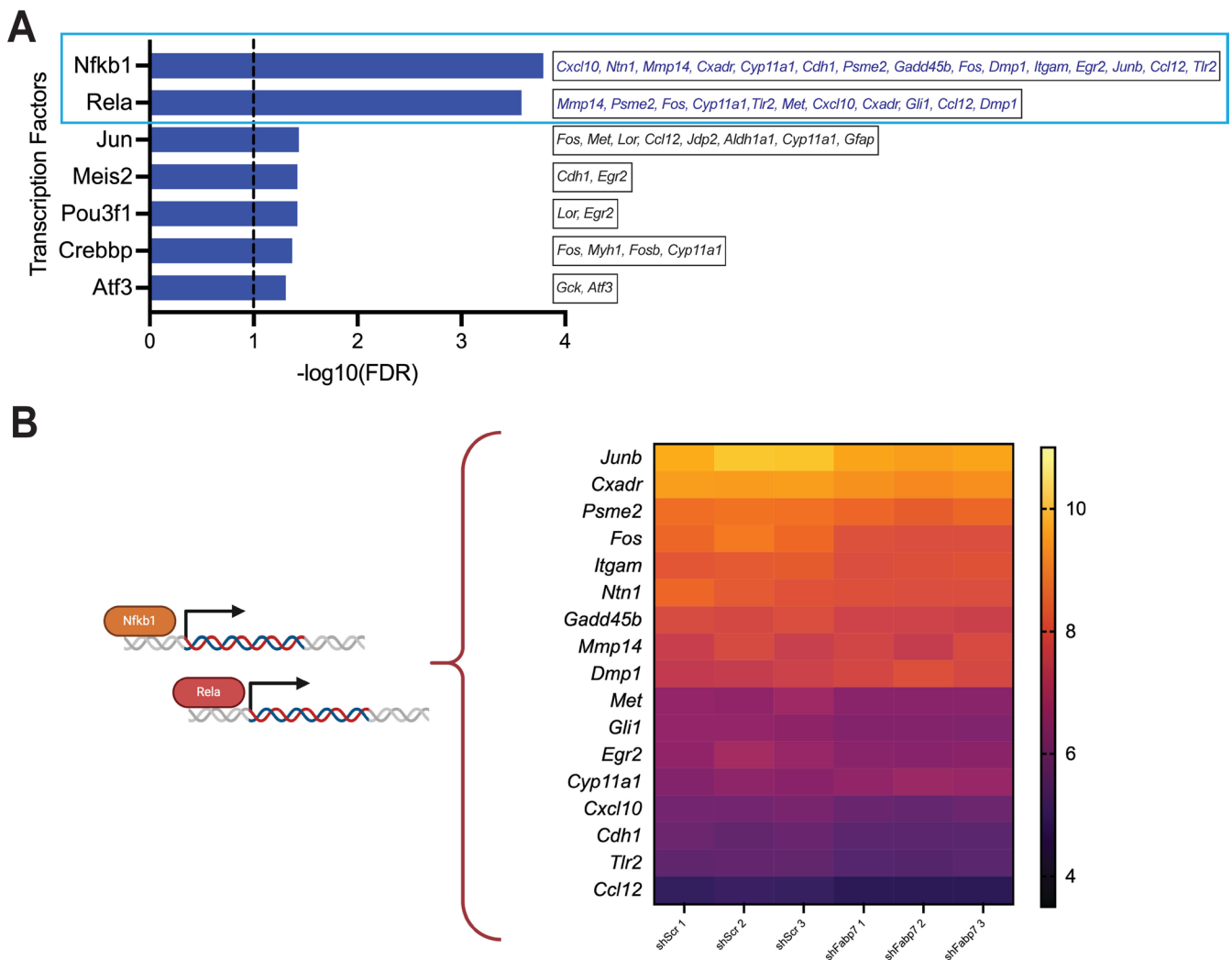


FIGURE 8 | Knockdown of FABP7 expression reduces NF- κ B-mediated transcriptional activity in a mouse model of neuroinflammation. RNA sequencing analysis was performed in RNA isolated from the cerebral cortex of AAV-PHP.eB-Gfap-GFP-shFABP7 or control AAV-PHP.eB-Gfap-GFP-shScr vector injected mice and treated with LPS as indicated in Figure 5. Identified transcripts with a p Adj < 0.05 and at least a 1.5-fold change in expression were included in the subsequent analysis. (A) Over-represented Transcription Factors (TF) identified using TRRUST v2 search of candidate key regulators of differentially expressed protein-coding transcripts. Statistical significance was established at Benjamini-Hochberg false discovery rate (FDR) < 0.05. (B) Heatmap of normalized log₂ expression counts for the transcripts corresponding to the top two TF identified in (A). All transcripts have a p Adj < 0.05.

downregulated in shFABP7-LPS mice when compared with shScr-LPS treated mice. These include *Serpina3n*, *Fcgr2b*, *Ifitm3*, *C4b*, and *Gfap*; transcripts present in all astrocytic clusters previously described by Hasel et al. (Hasel et al. 2021) and significantly downregulated in our data set (Figure S2). These data indicate that silencing FABP7 in the context of an inflammatory stimulus decreases transcriptional changes linked to neuroinflammation.

FABP7 expression is specifically upregulated by reactive astrocytes in multiple pathological conditions, including trauma and neurodegenerative diseases (Hamilton et al. 2024b; Killoy et al. 2020; Kipp et al. 2011; Rui et al. 2019; Sharifi et al. 2011; Teunissen et al. 2011; White et al. 2010). Our previously published data (Hamilton et al. 2024b; Killoy et al. 2020) and the data presented here show that increased FABP7 expression in

astrocytes favors the development of a proinflammatory phenotype, while downregulation of FABP7 reduces the response of astrocytes to inflammatory stimuli. As a more complete understanding of the mechanism governing this observation develops, strategies targeting specific FABP7-dependent pathways may represent promising therapeutic targets to modulate neuroinflammation.

Author Contributions

M.B., D.E., G.B., H.L.H., J.S.S., M.P., and M.R.V. performed experiments. M.B., M.P., and M.R.V. analyzed data. M.B., M.P., and M.R.V. wrote the paper. All authors reviewed and approved the content of the manuscript.

Acknowledgments

This study was funded by NIH grant R01NS122973 and R01NS132760.

Conflicts of Interest

The authors declare no conflicts of interest.

Data Availability Statement

The data that support the findings of this study are available from the corresponding author upon reasonable request.

References

- Bagga, D., L. Wang, R. Farias-Eisner, J. A. Glaspy, and S. T. Reddy. 2003. "Differential Effects of Prostaglandin Derived From Omega-6 and Omega-3 Polyunsaturated Fatty Acids on COX-2 Expression and IL-6 Secretion." *Proceedings of the National Academy of Sciences of the United States of America* 100, no. 4: 1751–1756. <https://doi.org/10.1073/pnas.0334211100>.
- Balendiran, G. K., F. Schnutgen, G. Scapin, et al. 2000. "Crystal Structure and Thermodynamic Analysis of Human Brain Fatty Acid-Binding Protein." *Journal of Biological Chemistry* 275, no. 35: 27045–27054. <https://doi.org/10.1074/jbc.M003001200>.
- Banks, W. A., and S. M. Robinson. 2010. "Minimal Penetration of Lipopolysaccharide Across the Murine Blood-Brain Barrier." *Brain, Behavior, and Immunity* 24, no. 1: 102–109. <https://doi.org/10.1016/j.bbi.2009.09.001>.
- Cassina, P., H. Peluffo, M. Pehar, et al. 2002. "Peroxyntirite Triggers a Phenotypic Transformation in Spinal Cord Astrocytes That Induces Motor Neuron Apoptosis." *Journal of Neuroscience Research* 67, no. 1: 21–29. <https://doi.org/10.1002/jnr.10107>.
- Catorce, M. N., and G. Gevorkian. 2016. "LPS-Induced Murine Neuroinflammation Model: Main Features and Suitability for Pre-Clinical Assessment of Nutraceuticals." *Current Neuropharmacology* 14, no. 2: 155–164. <https://doi.org/10.2174/1570159x14666151204122017>.
- Chen, S. H., E. A. Oyarzabal, Y. F. Sung, et al. 2015. "Microglial Regulation of Immunological and Neuroprotective Functions of Astroglia." *Glia* 63, no. 1: 118–131. <https://doi.org/10.1002/glia.22738>.
- da Silva, A. A. F., M. B. Fiadeiro, L. I. Bernardino, C. S. P. Fonseca, G. M. F. Baltazar, and A. C. B. Cristovao. 2024. "Lipopolysaccharide-Induced Animal Models for Neuroinflammation—An Overview." *Journal of Neuroimmunology* 387: 578273. <https://doi.org/10.1016/j.jneuroim.2023.578273>.
- DiSabato, D. J., N. Quan, and J. P. Godbout. 2016. "Neuroinflammation: The Devil Is in the Details." *Journal of Neurochemistry* 139, no. Suppl 2: 136–153. <https://doi.org/10.1111/jnc.13607>.
- Elsherbiny, M. E., M. Emara, and R. Godbout. 2013. "Interaction of Brain Fatty Acid-Binding Protein With the Polyunsaturated Fatty Acid Environment as a Potential Determinant of Poor Prognosis in Malignant Glioma." *Progress in Lipid Research* 52, no. 4: 562–570. <https://doi.org/10.1016/j.plipres.2013.08.004>.
- Garin-Shkolnik, T., A. Rudich, G. S. Hotamisligil, and M. Rubinstein. 2014. "FABP4 Attenuates PPARgamma and Adipogenesis and Is Inversely Correlated With PPARgamma in Adipose Tissues." *Diabetes* 63, no. 3: 900–911. <https://doi.org/10.2337/db13-0436>.
- Gorina, R., M. Font-Nieves, L. Marquez-Kisinousky, T. Santalucia, and A. M. Planas. 2011. "Astrocyte TLR4 Activation Induces a Proinflammatory Environment Through the Interplay Between MyD88-Dependent NFkappaB Signaling, MAPK, and Jak1/Stat1 Pathways." *Glia* 59, no. 2: 242–255. <https://doi.org/10.1002/glia.21094>.
- Hamilton, H. L., M. Akther, S. Anis, C. B. Colwell, M. R. Vargas, and M. Pehar. 2024a. "Nicotinamide Adenine Dinucleotide Precursor Supplementation Modulates Neurite Complexity and Survival in Motor Neurons From Amyotrophic Lateral Sclerosis Models." *Antioxidants & Redox Signaling* 41, no. 7–9: 573–589. <https://doi.org/10.1089/ars.2023.0360>.
- Hamilton, H. L., N. A. Kinscherf, G. Balmer, et al. 2024b. "FABP7 Drives an Inflammatory Response in Human Astrocytes and Is Upregulated in Alzheimer's Disease." *Geroscience* 46, no. 2: 1607–1625. <https://doi.org/10.1007/s11357-023-00916-0>.
- Han, H., J. W. Cho, S. Lee, et al. 2018. "TRRUST v2: An Expanded Reference Database of Human and Mouse Transcriptional Regulatory Interactions." *Nucleic Acids Research* 46, no. D1: D380–D386. <https://doi.org/10.1093/nar/gkx1013>.
- Harlan, B. A., K. M. Killoy, M. Pehar, L. Liu, J. Auwerx, and M. R. Vargas. 2020. "Evaluation of the NAD(+) Biosynthetic Pathway in ALS Patients and Effect of Modulating NAD(+) Levels in hSOD1-Linked ALS Mouse Models." *Experimental Neurology* 327: 113219. <https://doi.org/10.1016/j.expneurol.2020.113219>.
- Harlan, B. A., M. Pehar, K. M. Killoy, and M. R. Vargas. 2019. "Enhanced SIRT6 Activity Abrogates the Neurotoxic Phenotype of Astrocytes Expressing ALS-Linked Mutant SOD1." *FASEB Journal* 33, no. 6: 7084–7091. <https://doi.org/10.1096/fj.201802752R>.
- Harlan, B. A., M. Pehar, D. R. Sharma, G. Beeson, C. C. Beeson, and M. R. Vargas. 2016. "Enhancing NAD+ Salvage Pathway Reverts the Toxicity of Primary Astrocytes Expressing Amyotrophic Lateral Sclerosis-Linked Mutant Superoxide Dismutase 1 (SOD1)." *Journal of Biological Chemistry* 291, no. 20: 10836–10846. <https://doi.org/10.1074/jbc.M115.698779>.
- Hasel, P., I. V. L. Rose, J. S. Sadick, R. D. Kim, and S. A. Liddelow. 2021. "Neuroinflammatory Astrocyte Subtypes in the Mouse Brain." *Nature Neuroscience* 24, no. 10: 1475–1487. <https://doi.org/10.1038/s41593-021-00905-6>.
- Helledie, T., M. Antonius, R. V. Sorensen, et al. 2000. "Lipid-Binding Proteins Modulate Ligand-Dependent Trans-Activation by Peroxisome Proliferator-Activated Receptors and Localize to the Nucleus as Well as the Cytoplasm." *Journal of Lipid Research* 41, no. 11: 1740–1751.
- Holm, T. H., D. Draeby, and T. Owens. 2012. "Microglia Are Required for Astroglial Toll-Like Receptor 4 Response and for Optimal TLR2 and TLR3 Response." *Glia* 60, no. 4: 630–638. <https://doi.org/10.1002/glia.22296>.
- Huang, H., O. Starodub, A. McIntosh, A. B. Kier, and F. Schroeder. 2002. "Liver Fatty Acid-Binding Protein Targets Fatty Acids to the Nucleus. Real Time Confocal and Multiphoton Fluorescence Imaging in Living Cells." *Journal of Biological Chemistry* 277, no. 32: 29139–29151. <https://doi.org/10.1074/jbc.M202923200>.
- Hughes, M. L., B. Liu, M. L. Halls, et al. 2015. "Fatty Acid-Binding Proteins 1 and 2 Differentially Modulate the Activation of Peroxisome Proliferator-Activated Receptor α in a Ligand-Selective Manner." *Journal of Biological Chemistry* 290, no. 22: 13895–13906. <https://doi.org/10.1074/jbc.M114.605998>.
- Johansson, J. U., S. Pradhan, L. A. Lokteva, et al. 2013. "Suppression of Inflammation With Conditional Deletion of the Prostaglandin E2 EP2 Receptor in Macrophages and Brain Microglia." *Journal of Neuroscience* 33, no. 40: 16016–16032. <https://doi.org/10.1523/JNEUROSCI.2203-13.2013>.
- Kagawa, Y., Y. Yasumoto, K. Sharifi, et al. 2015. "Fatty Acid-Binding Protein 7 Regulates Function of Caveolae in Astrocytes Through Expression of Caveolin-1." *Glia* 63, no. 5: 780–794. <https://doi.org/10.1002/glia.22784>.
- Kannan-Thulasiraman, P., D. D. Seachrist, G. H. Mahabeshwar, M. K. Jain, and N. Noy. 2010. "Fatty Acid-Binding Protein 5 and PPARbeta/Delta Are Critical Mediators of Epidermal Growth Factor Receptor-Induced Carcinoma Cell Growth." *Journal of Biological Chemistry* 285, no. 25: 19106–19115. <https://doi.org/10.1074/jbc.M109.099770>.

- Killoy, K. M., B. A. Harlan, M. Pehar, and M. R. Vargas. 2020. "FABP7 Upregulation Induces a Neurotoxic Phenotype in Astrocytes." *Glia* 68, no. 12: 2693–2704. <https://doi.org/10.1002/glia.23879>.
- Killoy, K. M., B. A. Harlan, M. Pehar, and M. R. Vargas. 2022. "NR1D1 Downregulation in Astrocytes Induces a Phenotype That Is Detrimental to Cocultured Motor Neurons." *FASEB Journal* 36, no. 4: e22262. <https://doi.org/10.1096/fj.202101275R>.
- Kipp, M., S. Gingele, F. Pott, et al. 2011. "BLBP-Expression in Astrocytes During Experimental Demyelination and in Human Multiple Sclerosis Lesions." *Brain, Behavior, and Immunity* 25, no. 8: 1554–1568. <https://doi.org/10.1016/j.bbi.2011.05.003>.
- Kurtz, A., A. Zimmer, F. Schnutgen, G. Bruning, F. Spener, and T. Muller. 1994. "The Expression Pattern of a Novel Gene Encoding Brain-Fatty Acid Binding Protein Correlates With Neuronal and Glial Cell Development." *Development* 120, no. 9: 2637–2649. <https://www.ncbi.nlm.nih.gov/pubmed/7956838>.
- Levi, L., Z. Wang, M. K. Doud, S. L. Hazen, and N. Noy. 2015. "Saturated Fatty Acids Regulate Retinoic Acid Signalling and Suppress Tumorigenesis by Targeting Fatty Acid-Binding Protein 5." *Nature Communications* 6: 8794. <https://doi.org/10.1038/ncomms9794>.
- Liddelew, S. A., K. A. Guttenplan, L. E. Clarke, et al. 2017. "Neurotoxic Reactive Astrocytes Are Induced by Activated Microglia." *Nature* 541, no. 7638: 481–487. <https://doi.org/10.1038/nature21029>.
- Linnerbauer, M., M. A. Wheeler, and F. J. Quintana. 2020. "Astrocyte Crosstalk in CNS Inflammation." *Neuron* 108, no. 4: 608–622. <https://doi.org/10.1016/j.neuron.2020.08.012>.
- Makowski, L., K. C. Brittingham, J. M. Reynolds, J. Suttles, and G. S. Hotamisligil. 2005. "The Fatty Acid-Binding Protein, aP2, Coordinates Macrophage Cholesterol Trafficking and Inflammatory Activity. Macrophage Expression of aP2 Impacts Peroxisome Proliferator-Activated Receptor Gamma and IkappaB Kinase Activities." *Journal of Biological Chemistry* 280, no. 13: 12888–12895. <https://doi.org/10.1074/jbc.M413788200>.
- Mita, R., M. J. Beaulieu, C. Field, and R. Godbout. 2010. "Brain Fatty Acid-Binding Protein and Omega-3/Omega-6 Fatty Acids: Mechanistic Insight Into Malignant Glioma Cell Migration." *Journal of Biological Chemistry* 285, no. 47: 37005–37015. <https://doi.org/10.1074/jbc.M110.170076>.
- Norden, D. M., P. J. Trojanowski, E. Villanueva, E. Navarro, and J. P. Godbout. 2016. "Sequential Activation of Microglia and Astrocyte Cytokine Expression Precedes Increased Iba-1 or GFAP Immunoreactivity Following Systemic Immune Challenge." *Glia* 64, no. 2: 300–316. <https://doi.org/10.1002/glia.22930>.
- Ouali Alami, N., C. Schurr, F. Olde Heuvel, et al. 2018. "NF- κ B Activation in Astrocytes Drives a Stage-Specific Beneficial Neuroimmunological Response in ALS." *EMBO Journal* 37, no. 16: e98697. <https://doi.org/10.15252/emboj.201798697>.
- Owada, Y., S. A. Abdelwahab, N. Kitanaka, et al. 2006. "Altered Emotional Behavioral Responses in Mice Lacking Brain-Type Fatty Acid-Binding Protein Gene." *European Journal of Neuroscience* 24, no. 1: 175–187. <https://doi.org/10.1111/j.1460-9568.2006.04855.x>.
- Owada, Y., T. Yoshimoto, and H. Kondo. 1996. "Spatio-Temporally Differential Expression of Genes for Three Members of Fatty Acid Binding Proteins in Developing and Mature Rat Brains." *Journal of Chemical Neuroanatomy* 12, no. 2: 113–122.
- Patani, R., G. E. Hardingham, and S. A. Liddelew. 2023. "Functional Roles of Reactive Astrocytes in Neuroinflammation and Neurodegeneration." *Nature Reviews Neurology* 19, no. 7: 395–409. <https://doi.org/10.1038/s41582-023-00822-1>.
- Perry, V. H., J. A. Nicoll, and C. Holmes. 2010. "Microglia in neurodegenerative disease." *Nature Reviews Neurology* 6, no. 4: 193–201. <https://doi.org/10.1038/nrneuro.2010.17>.
- Qin, L., X. Wu, M. L. Block, et al. 2007. "Systemic LPS Causes Chronic Neuroinflammation and Progressive Neurodegeneration." *Glia* 55, no. 5: 453–462. <https://doi.org/10.1002/glia.20467>.
- Ransohoff, R. M. 2016. "How Neuroinflammation Contributes to Neurodegeneration." *Science* 353, no. 6301: 777–783. <https://doi.org/10.1126/science.aag2590>.
- Rui, Q., H. Ni, X. Lin, et al. 2019. "Astrocyte-Derived Fatty Acid-Binding Protein 7 Protects Blood-Brain Barrier Integrity Through a Caveolin-1/MMP Signaling Pathway Following Traumatic Brain Injury." *Experimental Neurology* 322: 113044. <https://doi.org/10.1016/j.expneurol.2019.113044>.
- Saneto, R. P., and J. de Vellis. 1987. "Neuronal and Glial Cells: Cell Culture of the Central Nervous System." In *Neurochemistry: A Practical Approach*. IRL Press.
- Sharifi, K., Y. Morihira, M. Maekawa, et al. 2011. "FABP7 Expression in Normal and Stab-Injured Brain Cortex and Its Role in Astrocyte Proliferation." *Histochemistry and Cell Biology* 136, no. 5: 501–513. <https://doi.org/10.1007/s00418-011-0865-4>.
- Shen, Y., H. Qin, J. Chen, et al. 2016. "Postnatal Activation of TLR4 in Astrocytes Promotes Excitatory Synaptogenesis in Hippocampal Neurons." *Journal of Cell Biology* 215, no. 5: 719–734. <https://doi.org/10.1083/jcb.201605046>.
- Sofroniew, M. V. 2020. "Astrocyte Reactivity: Subtypes, States, and Functions in CNS Innate Immunity." *Trends in Immunology* 41, no. 9: 758–770. <https://doi.org/10.1016/j.it.2020.07.004>.
- Storch, J., and A. E. Thumser. 2010. "Tissue-Specific Functions in the Fatty Acid-Binding Protein Family." *Journal of Biological Chemistry* 285, no. 43: 32679–32683. <https://doi.org/10.1074/jbc.R110.135210>.
- Tan, N. S., N. S. Shaw, N. Vinckenbosch, et al. 2002. "Selective Cooperation Between Fatty Acid Binding Proteins and Peroxisome Proliferator-Activated Receptors in Regulating Transcription." *Molecular and Cellular Biology* 22, no. 14: 5114–5127.
- Teunissen, C. E., R. Veerhuis, J. De Vente, et al. 2011. "Brain-Specific Fatty Acid-Binding Protein Is Elevated in Serum of Patients With Dementia-Related Diseases." *European Journal of Neurology* 18, no. 6: 865–871. <https://doi.org/10.1111/j.1468-1331.2010.03273.x>.
- Thumser, A. E., J. B. Moore, and N. J. Plant. 2014. "Fatty Acid Binding Proteins: Tissue-Specific Functions in Health and Disease." *Current Opinion in Clinical Nutrition and Metabolic Care* 17, no. 2: 124–129. <https://doi.org/10.1097/MCO.0000000000000031>.
- White, R. E., D. M. McTigue, and L. B. Jakeman. 2010. "Regional Heterogeneity in Astrocyte Responses Following Contusive Spinal Cord Injury in Mice." *Journal of Comparative Neurology* 518, no. 8: 1370–1390. <https://doi.org/10.1002/cne.22282>.
- Wolfrum, C., C. M. Borrmann, T. Borchers, and F. Spener. 2001. "Fatty Acids and Hypolipidemic Drugs Regulate Peroxisome Proliferator-Activated Receptors Alpha- and Gamma-Mediated Gene Expression via Liver Fatty Acid Binding Protein: A Signaling Path to the Nucleus." *Proceedings of the National Academy of Sciences of the United States of America* 98, no. 5: 2323–2328. <https://doi.org/10.1073/pnas.051619898>.
- Yang, Q. Q., and J. W. Zhou. 2019. "Neuroinflammation in the Central Nervous System: Symphony of Glial Cells." *Glia* 67, no. 6: 1017–1035. <https://doi.org/10.1002/glia.23571>.
- Yu, S., L. Levi, G. Casadesus, G. Kunos, and N. Noy. 2014. "Fatty Acid-Binding Protein 5 (FABP5) Regulates Cognitive Function Both by Decreasing Anandamide Levels and by Activating the Nuclear Receptor Peroxisome Proliferator-Activated Receptor Beta/Delta (PPARbeta/Delta) in the Brain." *Journal of Biological Chemistry* 289, no. 18: 12748–12758. <https://doi.org/10.1074/jbc.M114.559062>.
- Yun, S. W., C. Leong, D. Zhai, et al. 2012. "Neural Stem Cell Specific Fluorescent Chemical Probe Binding to FABP7." *Proceedings of the*

National Academy of Sciences of the United States of America 109, no. 26: 10214–10217. <https://doi.org/10.1073/pnas.1200817109>.

Zamanian, J. L., L. Xu, L. C. Foo, et al. 2012. “Genomic Analysis of Reactive Astrogliosis.” *Journal of Neuroscience* 32, no. 18: 6391–6410. <https://doi.org/10.1523/JNEUROSCI.6221-11.2012>.

Zhang, Y., K. Chen, S. A. Sloan, et al. 2014. “An RNA-Sequencing Transcriptome and Splicing Database of Glia, Neurons, and Vascular Cells of the Cerebral Cortex.” *Journal of Neuroscience* 34, no. 36: 11929–11947. <https://doi.org/10.1523/JNEUROSCI.1860-14.2014>.

Supporting Information

Additional supporting information can be found online in the Supporting Information section.